Accepted Manuscript

A novel cereblon modulator for targeted protein degradation

Sung Ah Kim, Ara Go, Seung-Hyun Jo, Sun Jun Park, Young Uk Jeon, Ji Eun Kim, Heung Kyoung Lee, Chi Hoon Park, Chong-Ock Lee, Sung Goo Park, Pilho Kim, Byoung Chul Park, Sung Yun Cho, Sunhong Kim, Jae Du Ha, Jeong-Hoon Kim, Jong Yeon Hwang

PII: S0223-5234(19)30033-9

DOI: https://doi.org/10.1016/j.ejmech.2019.01.023

Reference: EJMECH 11030

To appear in: *European Journal of Medicinal Chemistry*

Received Date: 7 November 2018

Revised Date: 19 December 2018

Accepted Date: 10 January 2019

Please cite this article as: S.A. Kim, A. Go, S.-H. Jo, S.J. Park, Y.U. Jeon, J.E. Kim, H.K. Lee, C.H. Park, C.-O. Lee, S.G. Park, P. Kim, B.C. Park, S.Y. Cho, S. Kim, J. Du Ha, J.-H. Kim, J.Y. Hwang, A novel cereblon modulator for targeted protein degradation, *European Journal of Medicinal Chemistry* (2019), doi: https://doi.org/10.1016/j.ejmech.2019.01.023.

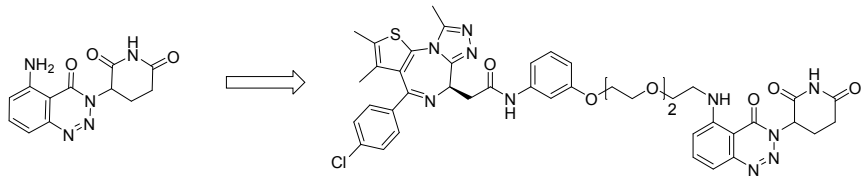

Novel CRBN ligand (TD-106)
-degradation of IKZF1/3

PROTAC (TD-428)
-degradation of BET proteins

A Novel Cereblon Modulator for Targeted Protein Degradation

Sung Ah Kim[1,2,#], Ara Go[3,#], Seung-Hyun Jo[1,2], Sun Jun Park[3], Young Uk Jeon[3], Ji Eun Kim[3], Heung Kyoung Lee [3], Chi Hoon Park[3, 4], Chong-Ock Lee[3], Sung Goo Park[1,2], Pilho Kim[3,4], Byoung Chul Park[1,5], Sung Yun Cho[3], Sunhong Kim [1,6], Jae Du Ha[*,3], Jeong-Hoon Kim[*,1,2], and Jong Yeon Hwang[*,3,4]

[1] Disease Target Structure Research Center, Korea Research Institute of Bioscience and Biotechnology, Daejeon 34141, Republic of Korea

[2] Department of Functional Genomics, University of Science and Technology, Daejeon 34113, Republic of Korea

[3]Therapeutics & Biotechnology Division, Korea Research Institute of Chemical Technology, Daejeon 34114, Republic of Korea

[4]Department of Medicinal Chemistry and Pharmacology, University of Science and Technology, Daejeon 34113, Republic of Korea

[5]Department of Bio-Analytical Science, University of Science and Technology, Daejeon 34113, Republic of Korea

[6] Department of Biomolecular Science, University of Science and Technology, Daejeon 34113, Republic of Korea

[#] These authors contributed equally to this study.

*Corresponding author. E-mail: jdha@krict.re.kr (J.D. Ha), jhoonkim@kribb.re.kr (J.-H. Kim), and jyhwang@krict.re.kr (J.H. Hwang)

Keywords: CRBN, BET, PROTAC, IMiDs

Abstract

Immunomodulatory drugs (IMiDs) exert anti-myeloma activity by binding to the protein cereblon (CRBN) and subsequently degrading IKZF1/3. Recently, their ability to recruit E3 ubiquitin ligase has been used in the proteolysis targeting chimera (PROTAC) technology. Herein, we design and synthesize a novel IMiD analog TD-106 that induces the degradation of IKZF1/3 and inhibits the proliferation of multiple myeloma cells *in vitro* as well as *in vivo*. Moreover, we demonstrate that TD-428, which comprises TD-106 linked to a BET inhibitor, JQ1 efficiently induce BET protein degradation in the prostate cancer cell line 22Rv1. Consequently, cell proliferation is inhibited due to suppressed C-MYC transcription. These results, therefore, firmly suggest that the newly synthesized IMiD analog, TD-106, is a novel CRBN modulator that can be used for targeted protein degradation.

1. Introduction

Immunomodulatory drugs (IMiDs), including thalidomide and its analogues, are a new class of anticancer agents with the glutarimide group, [1]. Thalidomide was developed and marketed as a sedative in the 1950s, but, was banned due to serious teratogenic effects in the early 1960s [2, 3]. Later on, it was demonstrated that thalidomide possessed anti-angiogenic and anti-inflammatory properties, and was consequently approved by the FDA for the treatment of multiple myeloma (MM) in 2006 [4, 5]. Although IMiDs were used for MM treatment, the mechanism underlying their pleotropic effects remained obscure for many years. By using affinity purification coupled with proteomic analysis, Ito *et al*., demonstrated that thalidomide specifically binds to cereblon (CRBN) and DNA damage-binding protein 1 (DDB1). Subsequently, CRBN, forms a Cullin Ring ligase (CRL) complex together with DDB1, CUL4, and RBX1 [6, 7]. Once bound to CRBN, IMiD promotes the degradation of IKZF1 and IKZF3 through the ubiquitination-dependent proteasome pathway [8, 9]. As thalidomide functioned successfully as an IMiD, next generation IMiDs, such as lenalidomide, pomalidomide, and CC122, were developed (Figure 1) [10] [1].

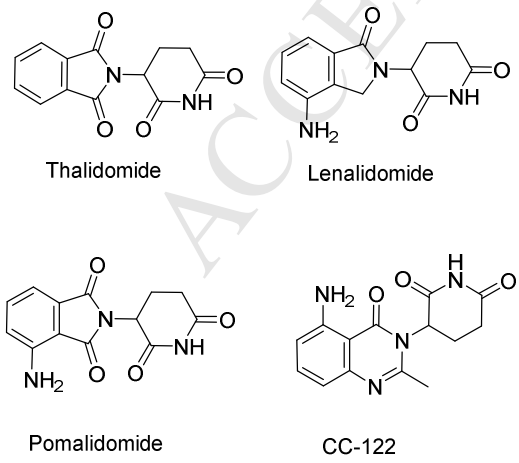

Figure 1. Known CRBN modulators (thalidomide, lenalidomide, pomalidomide, and CC-122).

The unique ability of IMiDs to bind to CRBN led to the development of the proteolysis targeting chimeras (PROTACs) technology. PROTAC is a bifunctional molecule with two ligands–one for the target protein, and the other for E3 ubiquitin ligases that induce proteasomal degradation of the target protein [11-15]. Several E3 ubiquitin ligases, including β-TrCP, MDM2, cIAP, VHL, and CRBN have been successfully applied for the degradation of various targets, such as FKBP12, ERα, AR, BET, BCR-ABL, BTK, and RIPK2 [16-20]. Of these, BRD4 is the most commonly-targeted protein in PROTAC technology. BRD4 is a member of the Bromodomain and Extra-Terminal domain (BET) family, which includes BRD2, BRD3, and BRDT [21-23]. The BET family recruits transcriptional regulatory complexes to acetylated chromatin, and control specific gene networks involved in cellular proliferation and cell cycle progression [24-26]. In particular, deregulation of BET protein activity, such as that of BRD4, is observed in cancer and inflammatory diseases, thereby making BET proteins attractive therapeutic targets [27, 28]. Therefore, several reports are available on the degradation of BET proteins in multiple cancer cells by highly potent PROTACs with thalidomide analogues or VHL ligands [21, 29-32].

Although PROTAC selectivity is theoretically dependent on the inhibitor warhead, it can also be influenced by the linker and the recruited E3 ligase [33, 34]. Therefore, discovery of novel E3 ligase ligands is important and necessary for PROTAC-based drug discovery. In the present study, we describe the synthesis and biological evaluation of a novel CRBN modulator (aminobenzotriazino glutarimide) and also validate its applicability in targeted protein degradation (Figure 2).

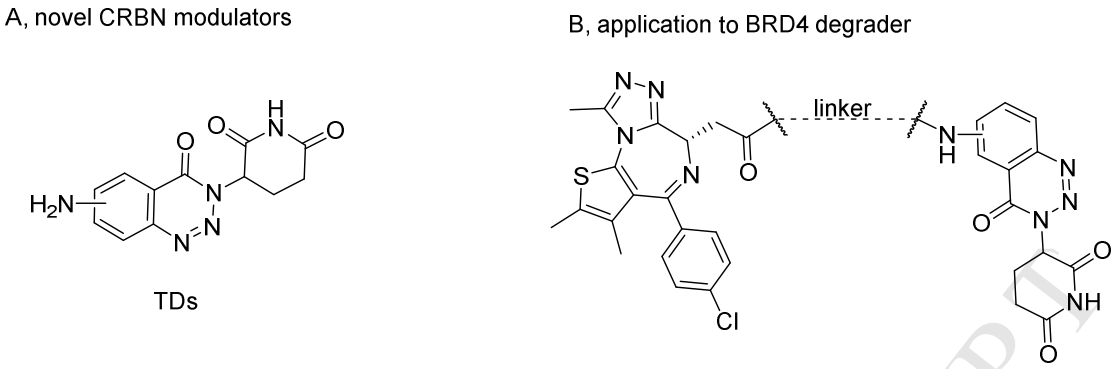

Figure 2. (A) Structure of a novel CRBN modulator (aminobenzotriazino glutarimide). (B) Application of the CRBN modulator in targeted protein degradation.

2. Results and Discussion

2.1. Chemistry

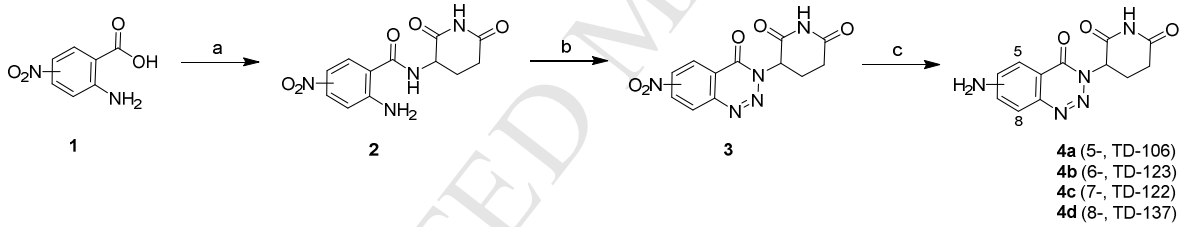

Scheme 1. Reagents and conditions; (a) 3-aminopiperidine-2,6-dione, EDCI, HOBt, DIPEA, DMF, rt; (b) $NaNO_2$, AcOH, rt; (c) Fe, AcOH, THF, rt.

Aminobenzotriazino glutarimides (TDs) **4** were synthesized as shown in Scheme 1. The reagent 2-amino-6-nitrobenzoic acid **1** reacts with 3-aminopiperidine-2,6-dione in the presence of EDCI, HOBt, and DIPEA at room temperature to give amide **2**. Cyclization of **2** was performed by treatment with $NaNO_2$ in AcOH, furnishing benzotriazinones **3**. The nitro functional group of **3** was reduced by treatment with iron in the presence of AcOH to give the desired aminobenzotriazino glutarimides **4**.

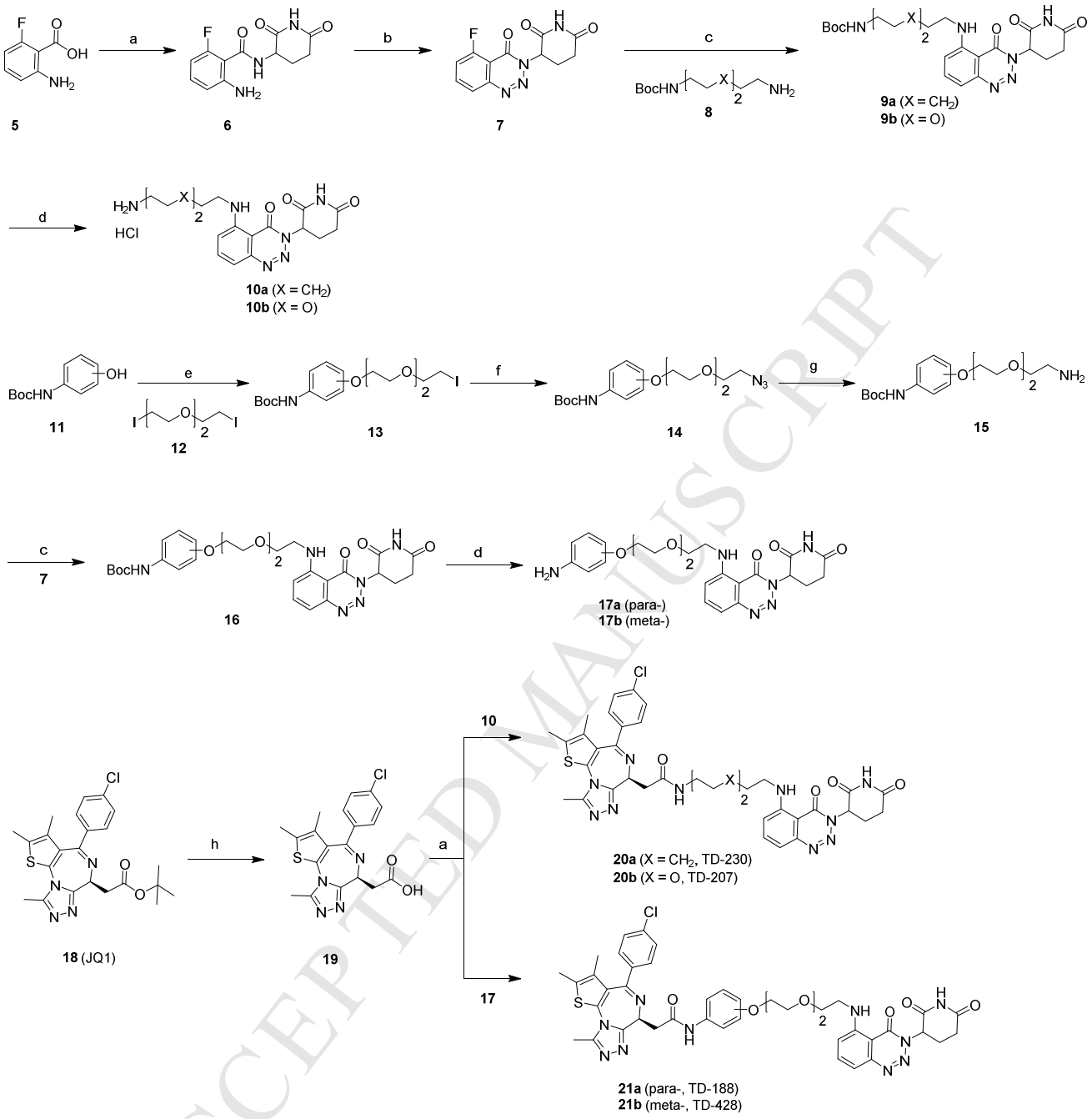

Scheme 2. Reagents and conditions; (a) 3-aminopiperidine-2,6-dione, EDCI, HOBt, DIPEA, DMF, rt; (b) $NaNO_2$, AcOH, rt; (c) DIPEA, DMF, 90 ℃; (d) 4 M HCl in dioxane, DCM, rt; (e) K_2CO_3, acetone, reflux; (f) NaN_3, DMF, 50 ℃; (g) $Pd(OH)_2$, H_2 (*g*), EtOH, rt; (h) TFA, DCM, rt; (i) EDCI, HOBt, DIPEA, DMF, rt.

Synthesis of BRD4 degraders is depicted in Scheme 2. For synthesizing a CRBN ligand, 5-fluorobenzotriazinone **7** was synthesized from 2-amino-6-fluorobenzoic acid

5 as per the same procedure described above. Nucleophilic substitution of **7** with different Boc-protected diamines **8** provided compounds **9**, which are transformed to intermediates **10** by TFA treatment. For intermediates **17** with aniline linker, Boc-aminophenols **11** were alkylated with diiodoalkane **12** to give compound **13**. Substitution reaction of **13** with NaN_3 provided azide **14** that was reduced to amine **15**. Similarly, condensation of **7** and the subsequent deprotection of Boc group provided intermediates **17**. Finally, reaction of the intermediates **10** and **17** with JQ1-acid **19** (generated from JQ1 by hydrolysis of *tert*-butylester) gave the desired BRD4 degraders **20** and **21**, respectively, via treatment with EDCI, HOBt, and DIPEA in DMF.

2.2. Biology

2.2.1. Identification of a novel CRBN modulator

To determine whether TDs (**4a-4d**) can induce the degradation of IKZF1/3 like IMiDs, NCI-H929 cells were treated with increasing amounts of TDs or pomalidomide. TD-106 (**4a**) induced the degradation of IKZF1/3 as much as pomalidomide did (Figure 3A), whereas the other analogs **4b-4d** showed no degradation (data not shown). Binding of target proteins with ligands improve their thermal stability. On this basis, we determined whether TD-106 directly binds to CRBN. At 53 °C, treatment with TD-106 and pomalidomide increased thermal stability in a dose dependent manner whereas treatment with DMSO did not (Figure 3B). Clinically, IMiDs are used to treat multiple myeloma as it induces cell cytotoxicity in multiple myeloma cell lines [35]. Therefore, we carried out the cytotoxicity assay with the NCI-H929 myeloma

cell line to see if TD-106 inhibits proliferation. Treatment of NCI-H929 with TD-106 or pomalidomide at similar concentrations (CC_{50} = 0.039 μM and 0.035 μM, respectively, Figure 3C) inhibited cell proliferation.

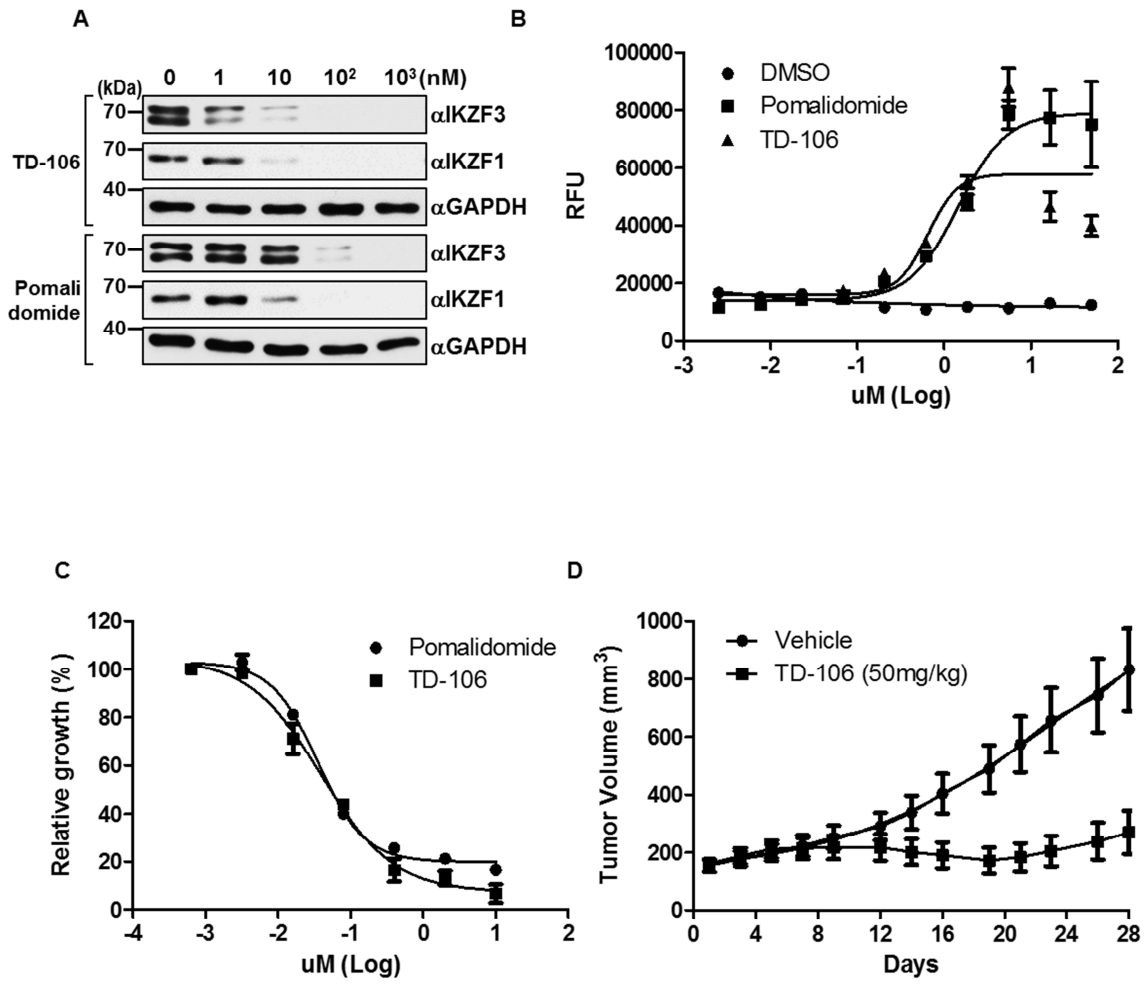

Figure 3. TD-106 is a novel CRBN modulator. **(**A) Degradation of IKZF1/3 by TD-106 in NCI-H929 cells. (B) Cellular thermal shift assay (CETSA) at 53 ℃ in HEK293 expressing CRBN-ePL. (C) Cytotoxicity assay of pomalidomide and TD-106 in NCI-H929 cells (D) Antitumor activity of TD-106 in TMD-8 xenograft model. Compounds were administered intraperitoneally (i.p.) to SCID mice at doses of 50 mg/kg q.d. for 14 days. Data are represented as the mean ± standard error (n = 6).

2.2.2. *In vivo* evaluation of TD-106 in a xenograft model

To determine the antitumor property of TD-106, an *in vivo* xenograft study was performed with TMD8 cell lines, which is an ABC (activated B-cell) subtype of DLBCL (diffuse large B-cell lymphoma). TMD8 cells were implanted subcutaneously into the right flanks of female SCID mouse, and drug treatment was initiated after tumor volumes reached approximately 150 mm^3. TD-106 or control (DMSO) was administered intraperitoneally to tumor-implanted mice in 20% PEG 400 and 3% Tween 80 in PBS (-) at doses of 50 mg/kg q.d. for the 14-day study duration. The drug treatment inhibited tumor growth during this duration. However, slight rebound tumor-growth was observed after discontinuation of the dosage (Figure 3D), indicating that TD-106 possesses anti-myeloma activity *in vivo*. No side effects or changes in body weight were observed during the study (data not shown).

2.2.3. BRD4 PROTACs with TD-106 induce BRD4 degradation and anti-proliferative effects on 22Rv1 cells

Recently, IMiDs have been used to degrade endogenous target proteins with PROTACs [36]. To determine if TD-106 could induce targeted protein degradation, we developed a series of bifunctional compounds containing TD-106 and JQ1, a BET inhibitor, with various linkers [31, 37]. Based on previous reports [29, 32, 38, 39], four degraders (**20** and **21**) were synthesized and, were examined for BRD4 degradation by immunoblotting in 22Rv1, the prostate cancer cell line. A dose titration experiment in 22Rv1 spanning 24 h showed that compounds **21**, bearing a phenyl ring in the linker, are better at degrading BRD4 than compounds **20**, which

have a linear alkyl linker (Figure 4A). Compounds **21a** (TD-188) and **21b** (TD-428) have the same molecular weight, but the linker was attached to different positions of the phenyl ring. Meta-substituted **21b** (DC_{50} = 0.32 nM) induced a more potent degradation of BRD4 than did ARV-825 (DC_{50} = 0.57 nM), a known BET degrader. However, the degradation activity of para-substituted **21a** (DC_{50} = 3.3 nM) was weaker than that of ARV-825 (Figure 4B). Indeed, **21b** is approximately 50 times more potent than **21a,** indicating that the potency depends not only on the length of the linker, but also on its attachment location. Next, we examined the effects of the BRD4 degraders on the cell proliferation in 22Rv1. As with earlier results, cytotoxicity was highest with **21b** (CC_{50} = 20.1 nM, Figure 4C). Like other BET degraders, **21b** induced the degradation of all the studied BET proteins (Supplementary Figure 1A)

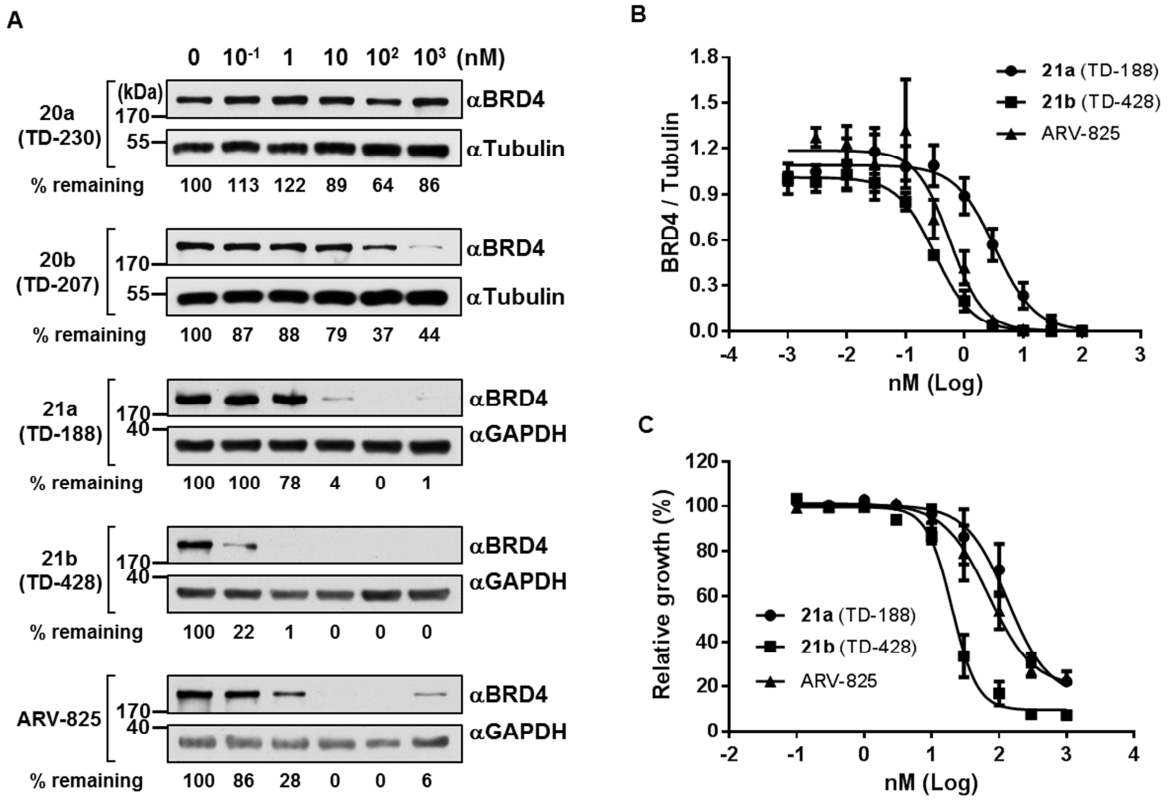

Figure 4. BET PROTACs with TD-106 induce BRD4 degradation (A and B) and

inhibit proliferation of 22RV1 cells (C).

2.2.4. Mechanistic characterization of BRD4 degradation by TD-428

Next, we investigated the mechanism of BRD4 degradation by TD-428. To determine if TD-428 mediated BRD4 degradation is dependent on UPS or CRL, the proteasome inhibitor Bortezomib, or the neddylation inhibitor MLN4924, was added along with TD-428. This completely inhibited BRD4 degradation, implying that BRD4 degradation by TD-428 is dependent on both UPS and CRL (Figure 5A). When endogenous CRBN was knocked down by specific siRNA, BRD4 levels remained unchanged in the presence of TD-428, suggesting that BRD4 degradation by TD-428 requires CRBN (Figure 5B). Moreover, TD-428-mediated BRD4 degradation was inhibited by addition of excess TD-106 or excess JQ1, indicating that proximity between BRD4 and CRBN is essential for BRD4 degradation (Figure 5C and 5D). As reported in other PROTAC compounds, TD-428 also facilitated the physical interaction between two unrelated proteins, BRD4 and CRBN (Figure 5E and Supplementary Figure 1B). Furthermore, TD-428 reduced C-MYC levels more efficiently than JQ1 (Figure 5F).

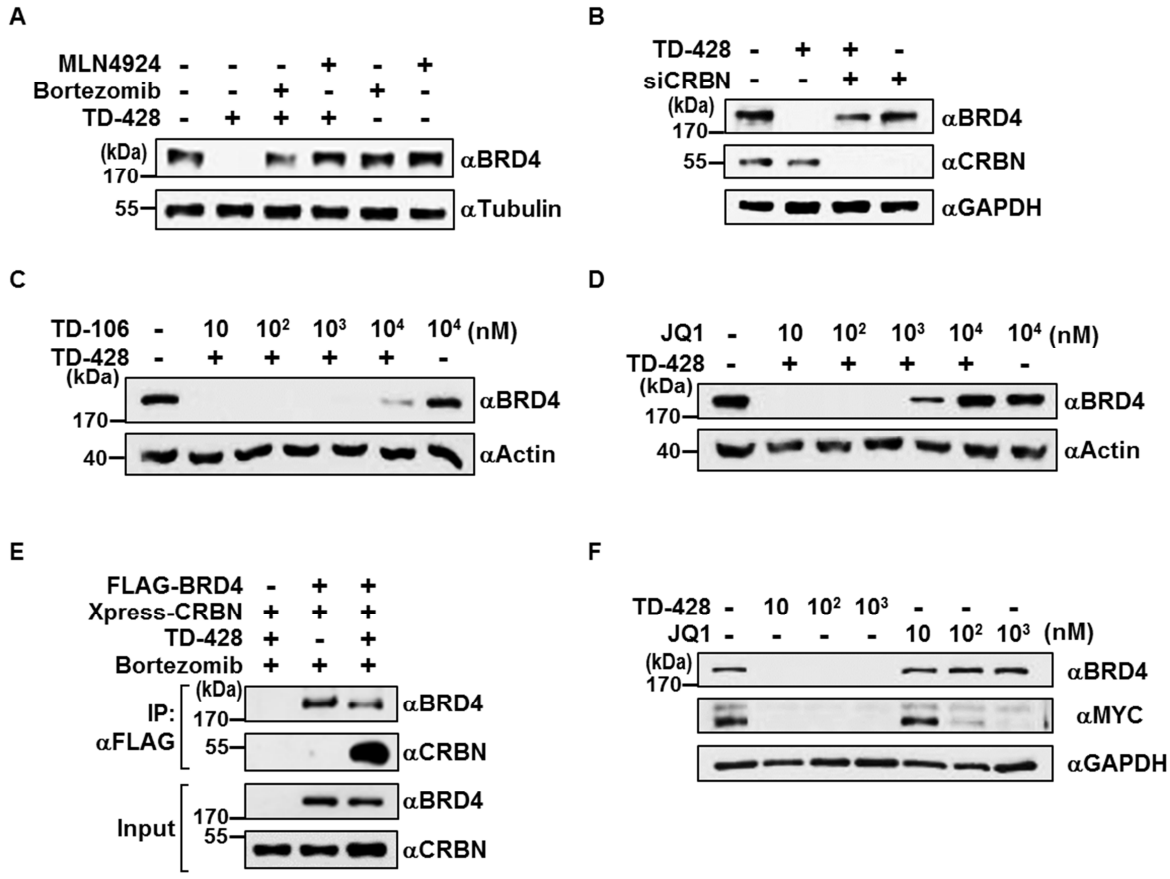

Figure 5. Mechanistic characterization of BRD4 degradation by TD-428. (A) UPS and CRL dependent BRD4 degradation by TD-428. (B) CRBN is required for TD428 mediated BRD4 degradation. (C) TD-428 mediated BRD4 degradation is inhibited by excessive TD-106 (D) TD-428 mediated BRD4 degradation is inhibited by excessive JQ1 (E) CRBN interacts with BRD4 in the presence of TD-428 (F) TD-428 reduced C-MYC levels more efficiently than JQ1

2.2.5. TD-428 is a highly specific BRD4 degrader

Biochemical characterization of TD-428 showed that it has a higher specificity for BRD4 than does ARV-825. However, the IKZF1/3 degradation efficiency of TD-428 is approximately 100-fold lower than that of ARV-825 (Figure 6). In addition, TD-428 lacked the hook effect, a typical characteristic of many PROTACs that prevents

target protein degradation at high doses of the compound [40].

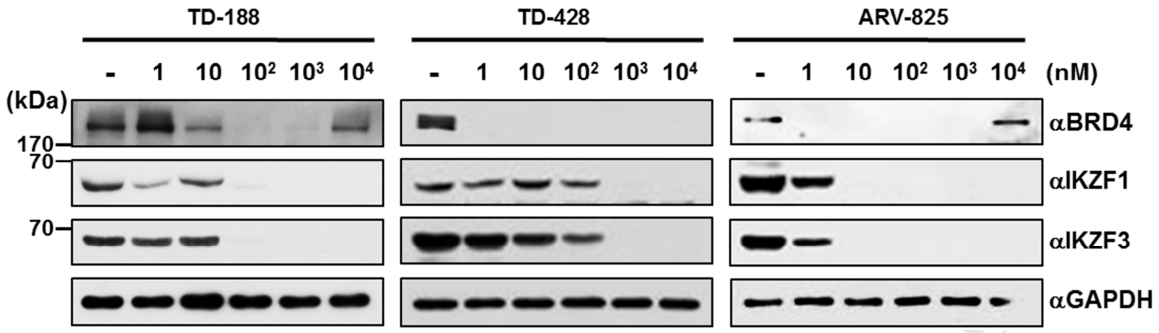

Figure 6. TD-428 is a more specific BRD4 degrader. U266 cells were treated with increasing concentration of TD188 (up to 10uM), TD428 (up to 10uM), or ARV825 (up to 10uM) for 12h. Cell lysates were prepared and analyzed by immunoblotting for BRD4, IKZF1, IKZF3 and GAPDH.

3. Conclusion

Targeted protein degradation by PROTAC is a powerful technology in drug discovery. Hijacking E3 ubiquitin ligases to target proteins by PROTAC is essential for its degradation. Although several E3 ubiquitin ligases, including β-TRCP, MDM2, cIAP, VHL, and CRBN have been successfully used in PROTACs, thalidomide analogs, CRBN ligands are the most widely used. In the present study, we discovered a novel CRBN modulator, TD-106. We showed that TD-106 induces the degradation of IKZF1/3 and inhibits the proliferation of multiple myeloma cells. In addition, we demonstrated that TD-428, the BRD4 degrader with TD-106, is highly specific for BET proteins and lacks the hook effect. Collectively, TD-106 as a novel CRBN modulator can be used for targeted protein degradation.

4. Experimental Section

4.1. Chemistry

All materials were obtained from commercial suppliers and used without further purification. Solvents in this study were dried using an aluminum oxide column. Thin-layer chromatography was performed on pre-coated silica gel 60 F254 plates (Merck, art. 5715). Purification of intermediates was carried out by normal phase column chromatography (MPLC, Silica gel 230-400 mesh). ^{1}H and ^{13}C NMR spectra were recorded with Bruker Avance 300 and 500, using $CDCl_3$ or other deuterated solvents as an internal standard. LC/MS analysis was performed the Agilent Technology 6130 Quadrupole LC/MS with electrospray ionization.The melting point was measured with Thomas-Hoover melting point apparatus.

*4.1.1. Synthesis of 2-amino-N-(2,6-dioxopiperidin-3-yl)-6-nitrobenzamide (**2a**)*

To a solution of 2-amino-6-nitrobenzoic acid (7.0 g, 38 mmol), 3-aminopiperidine-2,6-dione hydrogen chloride (25.0 g, 152 mmol), EDCl-HCl (8 .0g, 42 mmol), and HOBt (6.5 g, 42 mmol) in DMF (90 mL) was added DIPEA (21 mL, 121.6 mmol). The mixture was stirred at room temperature overnight. The reaction mixture was diluted with water and extracted with ethyl acetate. The organic layer was washed with brine, dried over Na_2SO_4, and concentrated. The crude compound **2a** was obtained as yellow solid (15 g) and used in the next step without further purification. ^{1}H NMR (300 MHz, DMSO-d_6) δ 10.99 (s, 1H), 9.02 (d, J = 8.2 Hz, 1H), 7.35–7.25 (m, 1H), 7.25–7.16 (m, 1H), 7.11–6.99 (m, 1H), 6.01 (s, 2H), 4.80–4.66 (m, 1H), 2.92–2.71 (m, 1H), 2.63–2.52 (m, 1H), 2.24–2.05 (m, 1H), 2.04–1.89 (m, 1H). ^{13}C NMR (101 MHz, DMSO-d_6) δ 173.0, 169.8, 151.5, 146.7, 144.0, 137.3, 131.7, 127.0, 111.0, 59.2, 31.1,

23.0 ;LC/MS $(M + H)^-$ (*m/z*) 292.9 ; LC/MS $(M + H)^-$ (*m/z*) 290.9 ; mp 230 ^oC

*Synthesis of 3-(5-nitro-4-oxobenzo[d][1,2,3]triazin-3(4H)-yl)piperidine-2,6-dione (**3a**)*

To a solution of **2a** (15 g) in AcOH added was sodium nitrite (2.7 g, 40 mmol) and stirred at room temperature for 1.5 h. The mixture was diluted with water and the precipitated white product was collected, washed with water, and dried to afford the product **3a** (7.0 g, 60%, 2 steps overallyield). ^1H NMR (300 MHz, DMSO-d_6) δ 11.25 (s, 1H), 8.53 (dd, *J* = 7.8, 1.5 Hz, 1H), 8.44–8.26 (m, 2H), 6.11–5.91 (m, 1H), 3.03–2.86 (m, 1H), 2.76–2.56 (m, 2H), 2.38–2.22 (m, 1H). ^{13}C NMR (101 MHz, DMSO-d_6) δ 173.6, 173.4, 165.3, 147.6, 147.6, 130.3, 120.9, 116.0, 111.1, 49.9, 31.4, 23.8 ;LC/MS $(M + H)^-$ (*m/z*) 303.9; LC/MS $(M + H)^-$ (*m/z*) 301.9 ; mp 265 ^oC

*4.1.2. Synthesis of 3-(5-amino-4-oxobenzo[d][1,2,3]triazin-3(4H)-yl)piperidine-2,6-dione (**4a**)*

To a suspension of **3a** (1.0 g, 3.2 mmol) in a mixture of AcOH (25 mL) and THF (25 mL) was added iron powder (1.0 g). The mixture was stirred at room temperature overnight. The reaction mixture was filtered and washed with ethyl acetate. The filtrate was washed with saturated aqueous $NaHCO_3$ and water, dried over $MgSO_4$, and concentrated under reduced pressure. The residue was purified by column chromatography to afford product **4a** (500 mg, 57%) as yellow solid. ^1H NMR (300 MHz, DMSO-d_6) δ 11.16 (s, 1H), 7.69 (t, *J* = 8.1 Hz, 1H), 7.27–7.15 (m, 3H), 7.01 (d, *J* = 8.3 Hz, 1H), 5.89–5.79 (m, 1H), 3.05–2.86 (m, 1H), 2.74–2.58 (m, 2H), 2.33–2.18 (m, 1H). ^{13}C NMR (125 MHz, DMSO) δ 172.8, 170.0, 156.8, 150.0, 145.0, 136.2, 116.7, 113.4, 101.6, 58.1 30.8, 22.6. ; LC/MS $(M + H)^-$ (*m/z*) 274.0; LC/MS $(M + H)^-$ (*m/z*) 272.0 ; mp 245 ^oC

*4.1.3. Synthesis of 2-amino-N-(2,6-dioxopiperidin-3-yl)-6-fluorobenzamide (**6**)*

To a solution of 2-amino-6-fluoro-benzoic acid (10 g, 64.46 mmol) in DMF (150 mL), EDCI·HCl (13.6 g, 70.90 mmol), HOBt (10.85 g , 70.90 mmol), and 3-amino pyridine-2,6-dione hydrogen chloride (10.85 g , 70.90 mmol), was added DIPEA (36.0 mL, 206.2 mmol). The mixture was stirred at room temperature for 9 h and was quenched with ice cold water. The precipitate was collected and washed with water and dried to afford **6** (15.6 g, 91%) as a bluish white solid; ^{1}H NMR (300 MHz, DMSO) δ 10.90 (s, 2H), 8.53 (dd, *J* = 8.2, 2.6 Hz, 2H), 7.16 – 7.05 (m, 2H), 6.52 (d, *J* = 8.2 Hz, 2H), 6.38 – 6.24 (m, 2H), 6.00 (s, 4H), 4.84 – 4.65 (m, 2H), 2.88 – 2.70 (m, 2H), 2.62 – 2.54 (m, 1H), 2.22 – 1.83 (m, 4H); LC/MS $(M + H)^-$ (*m/z*) 264.0; LC/MS $(M + H)^-$ (*m/z*) 274.8 flash point 250 ^{o}C.

*4.1.4. Synthesis of 3-(5-fluoro-4-oxobenzo[d][1,2,3]triazin-3(4H)-yl)piperidine-2,6-dione (**7**)*

To a solution of **6** (15 g, 56.6 mmol) in AcOH (400 mL) was added $NaNO_2$ (6.66 g , 96.1 mmol). The reaction mixture was stirred at room temperature for 2 h. After completion reaction, the reaction mixture was quenched with water (500 mL). The precipitant was collected, washed with water, and dried to afford **7** (11.2 g, 42%) as a white solid. ^{1}H NMR (300 MHz, DMSO-*d6*) δ 11.21 (s, 1H), 8.24–8.03 (m, 2H), 7.86–7.72 (m, 1H), 5.97 (dd, *J* = 12.1, 5.4 Hz, 1H), 2.96 (m, 1H), 2.76–2.58 (m, 2H), 2.35–2.16 (m, 1H); ^{13}C NMR (125 MHz, DMSO) δ 173.1, 170.1, 160.4, 158.3, 151.8 (d, *J* = 2.5 Hz), 145.4, 137.6 (d, *J* = 9.5 Hz), 125.0 (d, *J* = 4.0 Hz), 120.0 (d, *J* = 19.7 Hz), 58.0, 31.2, 23.0. flash point 270 ^{o}C.

4.1.5. Synthesis of tert-butyl (8-((3-(2,6-dioxopiperidin-3-yl)-4-oxo-3,4-

*dihydrobenzo[d][1,2,3]triazin-5-yl)amino)octyl)carbamate (**9a**)*

A solution of **7** (232 mg, 0.8 mmol), *tert*-butyl (8-aminooctyl)carbamate **8a** (227 mg, 0.9 mmol), and DIPEA (0.5 mL, 3 mmol) in DMF (10 mL) was reacted at 90 ℃ overnight. The reaction mixture was diluted with water and extracted with EtOAc. The organic layer was washed with brine, dried over $MgSO_4$, and concentrated. The residue was purified by column chromatography to give the compound **9a** (281 mg, 61%) as a yellow solid. ^{1}H NMR (300 MHz, $CDCl_3$) δ 8.35 (s, 1H), 8.24 – 8.11 (m, 1H), 7.70 (t, *J* = 8.2 Hz, 1H), 7.28 – 7.23 (m, 1H), 6.79 (d, *J* = 8.4 Hz, 1H), 5.76 – 5.65 (m, 1H), 4.58 (s, 1H), 3.31 – 3.19 (m, 2H), 3.17 – 3.07 (m, 2H), 3.02 – 2.69 (m, 3H), 2.43 – 2.26 (m, 1H), 1.81 – 1.69 (m, 2H), 1.57 – 1.35 (m, 15H); LC/MS $(M + H)^-$ (*m/z*) 498.9; mp 113–118 ^{o}C.

Similar procedure of **9a** was performed to give compound **9b** (13 mg, 34%) as a yellow solid. ^{1}H NMR (300 MHz, MeOD) δ 8.53 – 8.41 (m, 1H), 7.77 (t, *J* = 8.2 Hz, 1H), 7.29 – 7.19 (m, 1H), 6.98 (d, *J* = 8.5 Hz, 1H), 5.95 – 5.80 (m, 1H), 3.79 (t, *J* = 5.2 Hz, 2H), 3.74 – 3.61 (m, 4H), 3.61 – 3.51 (m, 2H), 3.51 – 3.39 (m, 2H), 3.28 – 3.18 (m, 2H), 3.02 – 2.76 (m, 3H), 2.41 – 2.30 (m, 1H), 1.41 (s, 9H); LC/MS $(M + H)^-$ (*m/z*) 498.9; mp 63–72 ^{o}C.

*4.1.6. Synthesis of 3-(5-((8-aminooctyl)amino)-4-oxobenzo[d][1,2,3]triazin-3(4H)-yl)piperidine-2,6-dione hydrogen chloride (**10a**)*

To a solution of **9a** (281 mg, 0.56 mmol) in DCM (3 mL) was added 4 N HCl in dioxane (0.1 mL) and stirred at room temperature for 1 h. The reaction mixture was concentrated under reduced pressure to afford **10a** (91%) as yellow solid. The next step was processed without purification. ^{1}H NMR (300 MHz, MeOD) δ 7.90 – 7.72 (m,

1H), 7.28 – 7.18 (m, 1H), 7.00 – 6.91 (m, 1H), 5.94 – 5.79 (m, 1H), 3.32 – 3.28 (m, 2H), 3.06 – 2.76 (m, 5H), 2.43 – 2.29 (m, 1H), 1.85 – 1.64 (m, 4H), 1.63 – 1.41 (m, 4H); LC/MS $(M + H)^+$ (*m/z*) 373.1, $(M + H)^-$ (*m/z*) 371.0; mp 110–125 ^oC.

Similar procedure of **10a** was performed to give compound **10b** (90%) as a yellow solid. ^1H NMR (400 MHz, MeOD) δ 7.79 (t, *J* = 8.2 Hz, 1H), 7.28 – 7.22 (m, 1H), 7.01 (d, *J* = 8.5 Hz, 1H), 5.91 – 5.81 (m, 1H), 3.81 (t, *J* = 5.1 Hz, 2H), 3.78 – 3.72 (m, 6H), 3.55 – 3.46 (m, 2H), 3.19 – 3.06 (m, 2H), 3.06 – 2.79 (m, 3H), 2.44 – 2.29 (m, 1H); LC/MS $(M + H)^+$ (*m/z*) 405.0, $(M + H)^-$ (*m/z*) 403.0; mp 58–63 ^oC.

*4.1.7. Synthesis of tert-butyl (4-(2-(2-(2-iodoethoxy)ethoxy)ethoxy)phenyl)carbamate (**13a**)*

A mixture of *tert*-butyl (4-hydroxyphenyl)carbamate **11** (522 mg, 2.5 mmol), **12** (4.62 g, 13 mmol), and K_2CO_3 (689 mg, 5.0 mmol) in acetone (15 mL) was refluxed overnight. The reaction mixture was diluted with water and extracted with EtOAc. The organic layer was washed with brine, dried over $MgSO_4$, and concentrated. The residue was purified by column chromatography to give the compound **13a** (322 mg, 75%) as a pale yellow oil. ^1H NMR (400 MHz, $CDCl_3$) δ 7.32 – 7.21 (m, 4H), 6.90 – 6.81 (m, 4H), 6.42 (s, 2H), 4.14 – 4.07 (m, 4H), 3.88 – 3.83 (m, 4H), 3.79 – 3.67 (m, 12H), 3.26 (t, *J* = 6.9 Hz, 4H), 1.51 (s, 19H). Similar procedure of **13a** was performed to give compound **13b** (13 mg, 34%) as a yellow solid. ^1H NMR (300 MHz, $CDCl_3$) δ 7.23 – 7.09 (m, 2H), 6.88 – 6.82 (m, 1H), 6.70 – 6.57 (m, 1H), 6.47 (s, 1H), 4.19 – 4.13 (m, 2H), 3.91 – 3.85 (m, 2H), 3.83 – 3.67 (m, 6H), 3.29 (t, *J* = 6.9 Hz, 2H), 1.54 (s, 9H).

*4.1.8. Synthesis of tert-butyl (4-(2-(2-(2-azidoethoxy)ethoxy)ethoxy)phenyl)carbamate (**14a**)*

A solution of **13a** (775 mg, 1.7 mmol), NaN_3 (335 mg, 5.2 mmol) in DMF (8 mL) was

reacted at 50 ℃ overnight. The reaction mixture was concentrated under reduced pressure to afford **14a.** The next step was processed without purification.

*4.1.9. Synthesis of tert-butyl (4-(2-(2-(2-aminoethoxy)ethoxy)ethoxy)phenyl)carbamate (**15a**)*

A solution of crude **14a** and $Pd(OH)_2$/carbon (16 mg) in EtOH (8 mL) was reacted at room temperature for 4 h under H_2 atmosphere. The reaction mixture was filtered through a pad of Celite and washed with EtOH. The filtrate was concentrated in vacuo to give the compound **15a** (424 mg, 73%) as a clear oil. ^{1}H NMR (300 MHz, $CDCl_3$) δ 7.28 – 7.22 (m, 2H), 6.90 – 6.83 (m, 2H), 6.41 (s, 1H), 4.19 – 4.04 (m, 2H), 3.93 – 3.81 (m, 2H), 3.76 – 3.70 (m, 2H), 3.69 – 3.64 (m, 2H), 3.54 (t, *J* = 5.2 Hz, 2H), 2.89 (t, *J* = 5.2 Hz, 2H), 2.18 (s, 3H), 1.52 (s, 9H); LC/MS $(M + H)^+$ (*m/z*) 341.1

Similar procedure of **15a** was performed to give compound **15b** (236 mg, quant.) as a yellow solid. ^{1}H NMR (300 MHz, $CDCl_3$) δ 7.18 (t, *J* = 8.1 Hz, 2H), 6.95 – 6.87 (m, 1H), 6.76 (s, 1H), 6.66 – 6.58 (m, 1H), 4.24 – 4.10 (m, 2H), 3.93 – 3.78 (m, 2H), 3.79 – 3.70 (m, 2H), 3.70 – 3.61 (m, 2H), 3.61 – 3.52 (m, 2H), 2.94 – 2.87 (m, 2H), 2.50 (s, 2H), 1.53 (s, 9H); LC/MS $(M + H)^+$ (*m/z*) 341.1

*4.1.10. Synthesis of tert-butyl (4-(2-(2-(2-((3-(2,6-dioxopiperidin-3-yl)-4-oxo-3,4-dihydrobenzo[d][1,2,3]triazin-5-yl)amino)ethoxy)ethoxy)ethoxy)phenyl)carbamate (**16a**)*

A mixture of **15a** (271 mg, 0.8 mmol), **7** (220 mg, 0.8 mmol), DIPEA (0.42 Ml, 2.4 mmol) in DMF (4 mL) was heated at 90 ℃ for 4 h. The reaction mixture was diluted with water and extracted with EtOAc. The organic layer was washed with brine, dried over $MgSO_4$, and concentrated. The residue was purified by column chromatography to give the crude compound **16a** (115 mg) as a yellow solid. ^{1}H NMR (300 MHz,

$CDCl_3$) δ 8.35 (t, *J* = 5.1 Hz, 1H), 8.25 (s, 1H), 7.67 (t, *J* = 8.2 Hz, 1H), 7.30 – 7.15 (m, 4H), 6.89 – 6.78 (m, 3H), 6.40 (s, 1H), 5.74 – 5.61 (m, 1H), 4.13 – 4.04 (m, 2H), 3.87 – 3.81 (m, 2H), 3.81 – 3.65 (m, 6H), 3.47 – 3.34 (m, 2H), 3.01 – 2.66 (m, 3H), 2.37 – 2.23 (m, 1H), 1.51 (s, 9H); LC/MS $(M + H)^+$ (*m/z*) 597.0, $(M + H)^-$ (*m/z*) 594.9; mp 80–88 ^oC

Similar procedure of **16a** was performed to give compound **16b** (259 mg, 62%) as a yellow solid. ^1H NMR (400 MHz, $CDCl_3$) δ 8.42 – 8.34 (m, 1H), 8.31 (s, 1H), 7.69 (t, *J* = 8.1 Hz, 1H), 7.29 – 7.25 (m, 1H), 7.18 – 7.12 (m, 1H), 7.10 (s, 1H), 6.88 – 6.81 (m, 2H), 6.68 – 6.56 (m, 2H), 5.77 – 5.65 (m, 1H), 4.20 – 4.09 (m, 2H), 3.94 – 3.85 (m, 2H), 3.83 – 3.66 (m, 6H), 3.50 – 3.35 (m, 2H), 3.01 – 2.70 (m, 4H), 2.38 – 2.29 (m, 1H), 1.53 (s, 9H); LC/MS $(M + H)^+$ (*m/z*) 597.0, $(M + H)^-$ (*m/z*) 594.9; mp 80–87 ^oC.

*4.1.11. Synthesis of 3-(5-((2-(2-(2-(4-aminophenoxy)ethoxy)ethoxy)ethyl)amino)-4-oxobenzo[d][1,2,3]triazin-3(4H)-yl)piperidine-2,6-dioneyl)piperidine-2,6-dione (**17a**)*

To a solution of **16a** (115 mg, 0.2 mmol) in DCM (5 mL) was added 4 M HCl in dioxane (2 mL) at room temperature for 1 h. The reaction mixture was concentrated and dissolved in DCM. The organic layer was neutralized with aqueous $NaHCO_3$, washed with brine, dried over $MgSO_4$, and concentrated. The residue was purified by column chromatography to give the compound **17a** (28 mg, 29%) as a yellow solid. ^1H NMR (300 MHz, $CDCl_3$) δ 9.18 (s, 1H), 8.38 – 8.27 (m, *J* = 5.0 Hz, 1H), 7.69 – 7.58 (m, *J* = 8.1 Hz, 1H), 7.26 – 7.13 (m, *J* = 7.7 Hz, 1H), 6.83 – 6.76 (m, *J* = 8.5 Hz, 1H), 6.71 (d, *J* = 8.8 Hz, 2H), 6.59 (d, *J* = 8.7 Hz, 2H), 5.76 – 5.60 (m, *J* = 11.5, 5.0 Hz, 1H), 4.11 – 3.94 (m, 2H), 3.87 – 3.77 (m, 2H), 3.77 – 3.65 (m, 6H), 3.56 (s, 2H), 3.47 – 3.34 (m, *J* = 10.4, 5.1 Hz, 2H), 2.91 – 2.61 (m, 3H), 2.33 – 2.15 (m, *J* = 11.3, 6.7 Hz, 1H); LC/MS $(M + H)^+$ (*m/z*) 497.0, $(M + H)^-$ (*m/z*) 494.9; mp 63–74 ^oC.

Similar procedure of **17a** was performed to give compound **17b** (105mg, 49%) as a yellow solid. ^{1}H NMR (300 MHz, $CDCl_3$) δ 8.52 (s, 1H), 8.37 (s, 1H), 7.68 (t, *J* = 8.1 Hz, 1H), 7.29 – 7.25 (m, 1H), 7.11 – 7.02 (m, 1H), 7.02 – 6.99 (m, 1H), 6.83 (d, *J* = 8.5 Hz, 1H), 6.47 – 6.34 (m, 2H), 5.77 – 5.66 (m, 1H), 4.13 – 4.01 (m, 2H), 3.91 – 3.83 (m, 2H), 3.83 – 3.68 (m, 6H), 3.49 – 3.36 (m, 2H), 2.99 – 2.67 (m, 3H), 2.38 – 2.20 (m, 1H); LC/MS $(M + H)^+$ (*m/z*) 497.0, $(M + H)^-$ (*m/z*) 494.9; mp 52–65 ^{o}C.

4.1.12. *Synthesis of (S)-2-(4-(4-chlorophenyl)-2,3,9-trimethyl-6H-thieno[3,2-f][1,2,4]triazolo[4,3-a][1,4]diazepin-6-yl)acetic acid (**19**)*

The JQ1 **18** (1 g, 2.2 mmol) was dissolved in 40% TFA/DCM solution (24 mL) and stirred at room temperature for 5 h. The reaction mixture was concentrated and dissolved in EtOAc. The organic layer was washed with water and brine, dried over $MgSO_4$, and concentrated. The residue was purified by column chromatography to give the compound **19** (900 mg, quant.) as a yellow solid. ^{1}H NMR (300 MHz, Chloroform-*d*) δ 7.45 (d, *J* = 8.6 Hz, 2H), 7.36 (d, *J* = 8.6 Hz, 2H), 6.36 (s, 2H), 4.63 (t, *J* = 6.8 Hz, 1H), 3.81 – 3.55 (m, 2H), 2.74 (s, 3H), 2.44 (s, 3H), 1.72 (s, 3H). LC/MS $(M + H)^+$ (*m/z*) 400.9, $(M + H)^-$ (*m/z*) 398.9;; mp 90–93 ^{o}C

4.1.13. Synthesis of 2-((S)-4-(4-chlorophenyl)-2,3,9-trimethyl-6H-thieno[3,2-f][1,2,4]triazolo[4,3-a][1,4]diazepin-6-yl)-N-(8-((3-(2,6-dioxopiperidin-3-yl)-4-oxo-3,4-dihydrobenzo[d][1,2,3]triazin-5-yl)amino)octyl)acetamide (**20a**, TD-230)

A mixture of **10a** (10 mg, 0.03 mmol), **19** (13 mg, 0.03 mmol), EDCI·HCl (6 mg, 0.03 mmol), HOBt (5 mg, 0.03 mmol), DIPEA (0.03 mL, 0.14 mmol) in DMF (1 mL) was stirred at room temperature for 4 h. The reaction mixture was diluted with water and

extracted with EtOAc. The organic layer was washed with brine, dried over $MgSO_4$, and concentrated. The residue was purified by column chromatography to give the compound **20a** (5 mg, 60%) as a yellow solid. ^{1}H NMR (300 MHz, $CDCl_3$) δ 9.06 (s, 1H), 8.94 (s, 1H), 8.23 – 8.11 (m, 2H), 7.73 – 7.64 (m, 2H), 7.40 (d, *J* = 8.4 Hz, 4H), 7.36 – 7.28 (m, 5H), 7.23 (d, *J* = 7.7 Hz, 2H), 6.85 – 6.72 (m, 4H), 5.79 – 5.62 (m, 2H), 4.64 (t, *J* = 7.0 Hz, 2H), 3.66 – 3.51 (m, 2H), 3.42 – 3.13 (m, 10H), 3.00 – 2.75 (m, 6H), 2.66 (s, 6H), 2.39 (s, 5H), 2.37 – 2.27 (m, 3H), 1.74 – 1.62 (m, 10H), 1.60 – 1.51 (m, 4H), 1.45 – 1.35 (m, 7H); ^{13}C NMR (101 MHz, $CDCl_3$) δ 171.23, 171.17, 170.49, 170.48, 168.28, 163.91, 157.76, 155.67, 149.90, 149.58, 145.70, 145.69, 136.73, 136.64, 136.50, 132.16, 130.89, 130.80, 130.45, 129.84, 128.68, 113.53, 111.60, 102.58, 102.54, 77.40, 77.08, 76.76, 58.28, 58.07, 54.54, 42.93, 42.89, 39.48, 39.42, 39.40, 31.08, 31.04, 29.31, 29.28, 28.44, 28.40, 26.70, 26.66, 26.49, 26.46, 23.13, 14.37, 13.08, 11.81; LC/MS $(M + H)^+$ (*m/z*) 754.9, $(M + H)^-$ (*m/z*) 752.9; mp 110–115 ^oC.

Synthesis of 2-((S)-4-(4-chlorophenyl)-2,3,9-trimethyl-6H-thieno[3,2-f][1,2,4]triazolo[4,3-a][1,4]diazepin-6-yl)-N-(2-(2-(2-((3-(2,6-dioxopiperidin-3-yl)-4-oxo-3,4-dihydrobenzo[d][1,2,3]triazin-5-yl)amino)ethoxy)ethoxy)ethyl)acetamide (**20b**, TD-207)

Similar procedure of **20a** was performed to give compound **20b** (47 mg, 88%) as a yellow solid. ^{1}H NMR (300 MHz, $CDCl_3$) δ 9.51 (s, 1H), 9.27 (s, 1H), 8.44 – 8.36 (m, 2H), 7.76 – 7.66 (m, 2H), 7.47 – 7.38 (m, 4H), 7.38 – 7.30 (m, 4H), 7.28 – 7.24 (m, 1H), 7.03 – 6.90 (m, 2H), 6.82 (d, *J* = 8.5 Hz, 2H), 5.72 – 5.52 (m, 2H), 4.67 (q, *J* = 6.8 Hz, 2H), 3.82 (t, *J* = 5.0 Hz, 4H), 3.75 – 3.28 (m, 25H), 2.97 – 2.75 (m, 6H), 2.67 (d, *J* = 3.8 Hz, 6H), 2.41 (s, 6H), 2.38 – 2.26 (m, 2H), 1.67 (d, *J* = 7.5 Hz, 6H); ^{13}C

NMR (101 MHz, $CDCl_3$) δ 171.20, 170.81, 170.71, 168.31, 168.22, 163.99, 163.89, 157.56, 155.61, 149.88, 149.82, 149.43, 149.40, 145.75, 145.71, 136.69, 136.40, 132.23, 130.95, 130.87, 130.73, 130.69, 130.43, 129.90, 129.88, 128.67, 128.65, 113.99, 111.61, 103.10, 77.35, 77.03, 76.72, 70.84, 70.77, 70.35, 70.22, 69.84, 69.79, 69.11, 69.02, 59.12, 58.70, 54.45, 54.41, 42.95, 39.59, 39.19, 39.15, 31.13, 31.10, 22.97, 14.38, 14.35, 13.09, 11.85, 11.83; LC/MS $(M + H)^+$ (*m/z*) 786.9, $(M + H)^-$ (*m/z*) 784.9; mp 115–118 ^oC

2-((S)-4-(4-chlorophenyl)-2,3,9-trimethyl-6H-thieno[3,2-f][1,2,4]triazolo[4,3-a][1,4]diazepin-6-yl)-N-(3-(2-(2-(2-((3-(2,6-dioxopiperidin-3-yl)-4-oxo-3,4-dihydrobenzo[d][1,2,3]triazin-5-yl)amino)ethoxy)ethoxy)ethoxy)phenyl)acetamide (**21a**, TD-188)

Similar procedure of **20a** was performed to give compound **21a** (27 mg, 36%) as a yellow solid. ^1H NMR (300 MHz, $CDCl_3$) δ 9.15 (d, *J* = 11.9 Hz, 1H), 8.97 (s, 0H), 8.87 (s, 1H), 8.46 – 8.34 (m, 1H), 7.67 (t, *J* = 8.1 Hz, 1H), 7.58 – 7.38 (m, 4H), 7.38 – 7.30 (m, 2H), 7.30 – 7.20 (m, 2H), 6.91 – 6.73 (m, 3H), 5.78 – 5.57 (m, 1H), 4.80 – 4.67 (m, 1H), 4.18 – 4.05 (m, 2H), 3.92 – 3.66 (m, 9H), 3.66 – 3.52 (m, 1H), 3.52 – 3.33 (m, 2H), 2.95 – 2.58 (m, 6H), 2.42 (s, 3H), 2.35 – 2.20 (m, 1H), 1.68 (s, 3H); ^{13}C NMR (101 MHz, $CDCl_3$) δ 171.12, 171.09, 168.50, 168.48, 168.37, 168.33, 157.59, 157.56, 155.46, 155.31, 150.15, 149.50, 145.61, 136.42, 131.73, 131.32, 131.07, 131.05, 130.12, 130.07, 128.76, 121.59, 121.57, 114.95, 114.90, 113.97, 111.71, 102.79, 102.77, 77.37, 77.05, 76.73, 70.87, 70.84, 70.72, 69.77, 69.26, 69.24, 67.83, 67.81, 54.54, 42.94, 39.95, 31.03, 31.00, 23.23, 14.42, 13.14, 11.83; LC/MS $(M + H)^+$ (*m/z*) 878.9, $(M + H)^-$ (*m/z*) 876.7; mp 160–165 ^oC

4.1.14. *Synthesis of 2-((S)-4-(4-chlorophenyl)-2,3,9-trimethyl-6H-thieno[3,2-f][1,2,4]triazolo[4,3-a][1,4]diazepin-6-yl)-N-(4-(2-(2-(2-((3-(2,6-dioxopiperidin-3-yl)-4-oxo-3,4-dihydrobenzo[d][1,2,3]triazin-5-yl)amino)ethoxy)ethoxy)ethoxy)phenyl)acetamide* (**21b**, TD-428)

Similar procedure of **20a** was performed to give compound **21b** (20 mg, 30%) as a yellow solid. ^{1}H NMR (300 MHz, $CDCl_3$) δ 9.58 – 9.39 (m, 2H), 8.38 – 8.27 (m, 1H), 7.66 – 7.54 (m, 1H), 7.37 (d, *J* = 8.2 Hz, 2H), 7.29 – 7.24 (m, 2H), 7.21 – 7.15 (m, 1H), 7.15 – 7.01 (m, 2H), 6.75 (d, *J* = 8.5 Hz, 1H), 6.61 – 6.52 (m, 1H), 5.71 – 5.60 (m, 1H), 4.73 (t, *J* = 7.0 Hz, 1H), 4.12 – 4.00 (m, 2H), 3.84 – 3.77 (m, 2H), 3.74 – 3.55 (m, 8H), 3.43 – 3.30 (m, 2H), 2.80 – 2.70 (m, 2H), 2.67 (s, 3H), 2.36 (s, 4H), 1.63 (s, 4H), 1.38 – 1.11 (m, 2H); ^{13}C NMR (101 MHz, $CDCl_3$) δ 171.61, 171.56, 169.10, 168.80, 168.67, 164.13, 159.04, 157.52, 155.63, 155.61, 150.11, 150.09, 149.43, 145.54, 139.69, 136.73, 136.45, 136.35, 132.13, 132.12, 131.00, 130.89, 130.43, 130.41, 129.98, 129.39, 128.62, 113.77, 112.35, 111.68, 110.66, 110.61, 106.05, 105.93, 102.71, 77.55, 77.23, 76.92, 70.75, 70.74, 70.68, 70.66, 69.75, 69.17, 67.38, 57.49, 57.39, 54.45, 54.40, 42.84, 40.01, 30.99, 23.19, 23.16, 14.41, 13.09, 11.82; LC/MS $(M + H)^+$ (*m/z*) 878.9, $(M + H)^-$ (*m/z*) 876.7; mp 109–111 ^{o}C

Biology

4.1.15. Antibodies and reagents

Anti-BRD4 antibody (#13440), IKZF1 antibody (#9034) and IKZF3 antibody (#151035) were obtained from Cell Signaling Technology. Anti-CRBN antibody (HPA045910) and Anti-Flag M2 Magnetic Bead (M8823) were obtained from Sigma Aldrich. DBeQ (4417) was obtained from Tocris Bioscience. Anti-HA Magnetic Bead

(88837) was obtained from Thermo Scientific. MLN4924 (505477) was obtained from Calbiochem, Bortezomib (S1013) was obtained from Selleckchem.

4.1.16. Cell culture

HEK293T cell was maintained in Dulbecco's Modified Eagle's Medium (DMEM, Gibco) supplemented with 10% fetal bovine serum (FBS, Gibco), penicillin 100units/ml, streptomycin 100μg/ml and amphotericin B 0.25μg/ml (Gibco) in a humidified atmosphere of 5% CO_2 in air at 37 °C. 22Rv1 cell was maintained in RPMI-1640 Medium (Gibco) supplemented with 10% fetal bovine serum (FBS, Gibco), penicillin 100 units/mL, streptomycin 100 μg/mL and amphotericin B 0.25 μg/mL (Gibco) in a humidified atmosphere of 5% CO_2 in air at 37 °C. H929 cell was maintained in RPMI-1640 Medium (Gibco) supplemented with 10% fetal bovine serum (FBS, Gibco), penicillin 100 units/mL, streptomycin 100 μg/mL, amphotericin B 0.25 μg/mL (Gibco) and 2-mercaptoethanol 0.05 mM (Sigma) in a humidified atmosphere of 5% CO_2 in air at 37 °C.

4.1.17. Plasmid constructs and transfection

Xpress-CRBN, HA-CRBN and FLAG-BRD4 were cloned using Infusion cloning. Cells were transfected with various plasmids using X-treamGENE HP DNA Transfection Reagent (Roche) according to the manufacturer's instruction.

4.1.18. RNA interference

siRNA against CRBN (51185) and negative control siRNA (SN-1003) were obtained from Bioneer. For RNA interference, cells were transfected with siRNAs using Lipofectamine RNAiMAX Transfection Reagent (Invitrogen) according to the manufacturer's instruction. After 48h incubation, TD428 was treated for 12h. And cells were harvested and analyzed.

4.1.19. Immunoprecipitation and immunoblotting

Cells were lysed using lysis buffer (50 mM HEPES KOH pH 7.4, 40 mM NaCl, 1 mM EDTA, 1 mM EGTA, 10 mM sodium pyrophosphate, 10 mM sodium β-glycerophosphate, 50 mM NaF, 1 mM $NaVO_4$, 1% Triton X-100) containing protease inhibitor (05056489001, Roche). The lysate was incubated for 10 min on ice and clarified by centrifuging at 13,000 rpm, 4°C for 10 min. The supernatant was quantified and incubated with beads at 4°C for 3h. After incubation, beads were washed twice in lysis buffer and triplets in wash buffer (50 mM HEPES KOH pH 7.4, 500 mM NaCl, 1 mM EDTA, 1 mM EGTA, 10 mM sodium pyrophosphate, 10 mM sodium β-glycerophosphate, 50 mM NaF, 1 mM $NaVO_4$, 1% Triton X-100, protease inhibitor). Elution was performed using SDS Sample buffer (40 mM Tris HCl pH 6.8, 2% SDS, 0.05% bromophenol blue, 5% glycerol, 2.8 M mercaptoethanol) and samples were separated using SDS-PAGE. After transfer to NC membrane, immunoblotting was performed using the indicated antibodies.

4.1.20. Cellular Thermal Shift Assay (CESTA)

For the cell lysate CETSA experiments, cultured HEK293 cells were harvested and washed with PBS. The cells were diluted in Assay Medium (DMEM plus 10% FBS) to $1.25*10^5$/mL. 5xDMSO, 5xPomalidomide (up to 10 µM) and 5xTD106 (up to 10 µM) were split for 10 µL into assay plate. The cell lysates were split for 40 µL into assay plate with inhibitor. After 1 hour incubation in a humidified atmosphere of 5% CO_2 in air at 37°C, the assay plate were incubate at 53°C for 3 minutes using thermocycler (ProFlex, ThermoFisher Scientific). Sample in assay plate were transfer to 96-well white plate by 40 µL. Put the Master mix in each well for 60 µL (10 µL EA Reagent, 10 µL Lysis Buffer and 40 µL Substrate Reagent) and incubate for 1 hour at room temperature in dark. The 96-well white plate measured luminescence using luminometer (Victor, PerkinElmer). [44]

4.1.21. Proliferation Assay

22Rv1 cells (15,000/100 μL) were seeded in 96-well tissue culture white plates followed by addition of compound at indicated concentrations. After 72 hr, 100 μL per well of reconstituted CelTiter-Glo reagent (#G7572, Promega) was added and read on Luminometer (ProFlex, ThermoFisher Scientific). Relative cell growth was determined by comparing assay readings of treated cells with control DMSO-treated cells. NCI-H929 cells were seeded in 96-well plates at 30% confluency and exposed to chemicals the next day. After 72 h, WST-1 reagent was added and absorbance at 450 nm was measured using a Spectramax spectrophotometer (Molecular Devices, US) according to the manufacturer's instructions. The IC_{50}s were calculated using GraphPad Prism version 6 for Windows. The curves were fitted using a nonlinear regression model with a log (inhibitor) versus response formula.

4.1.22. In vivo xenograft assay

Female SCID (CB-17/IcrCri-scid) mice were obtained from Charles River of Japan. Animals were maintained under clean room conditions in sterile filter top cages and housed on high efficiency particulate air-filtered ventilated racks. Animals were received sterile rodent chow and water ad libitum. All of the procedures were conducted in accordance with guidelines approved by the Laboratory Animal Care and Use Committee of Korea Research Institute of Chemical Technology. TMD-8 cells were implanted subcutaneously into the right flank region of each mouse and allowed to grow to the designated size. Once tumors reached an average volume of about 150 mm3, mice were dosed via intraperitoneal daily with the indicated doses of TD-106 for 14 days. Mice were observed daily throughout the treatment period for signs of morbidity/mortality. Tumors were measured twice weekly using calipers, and volume was calculated using the formula: length x $width^2$ x 0.5. Body weight was

also assessed twice weekly. Statistical significances were evaluated by using Mann-Whitney U-test (a = 0.01).

Acknowledgements

This work was supported by the grant (CAP-15-11-KRICT) from National Research Council of Science and Technology, Ministry of Science, ICT, and future planning and the grant from KRIBB Initiative Program.

Author contributions

AG, SJP, YUK synthesized compounds. SAK, SHJ, JEK, HKL conducted biology experiments. CHP, COL, SGP, PK, BCP, SYC, SK designed and conducted some experiments. SAK, JDH, JHK, and JYH wrote the manuscript. JDH, JHK, and JYH contributed to experimental design and supervision.

Conflict of interest

The authors declare no conflict of interest.

References

[1] J.B. Bartlett, K. Dredge, A.G. Dalgleish, The evolution of thalidomide and its IMiD derivatives as anticancer agents, Nat Rev Cancer, 4 (2004) 314-322.
[2] A.L. Speirs, Thalidomide and congenital abnormalities, Lancet, 1 (1962) 303-305.
[3] P.M. Fullerton, M. Kremer, Neuropathy after intake of thalidomide (distaval), Br Med J, 2 (1961) 855-858.
[4] J.B. Marriott, G. Muller, A.G. Dalgleish, Thalidomide as an emerging immunotherapeutic agent, Immunol Today, 20 (1999) 538-540.
[5] F. van Rhee, M. Dhodapkar, J.D. Shaughnessy, Jr., E. Anaissie, D. Siegel, A. Hoering, J. Zeldis, B. Jenkins, S. Singhal, J. Mehta, J. Crowley, S. Jagannath, B. Barlogie, First thalidomide clinical trial in multiple myeloma: a decade, Blood, 112 (2008) 1035-1038.
[6] Y.X. Zhu, E. Braggio, C.X. Shi, K.M. Kortuem, L.A. Bruins, J.E. Schmidt, X.B. Chang, P. Langlais, M. Luo, P. Jedlowski, B. LaPlant, K. Laumann, R. Fonseca, P.L. Bergsagel, J. Mikhael, M. Lacy, M.D. Champion, A.K. Stewart, Identification of cereblon-binding proteins and relationship with response and survival after IMiDs in multiple myeloma, Blood, 124 (2014) 536-545.
[7] A. Thakurta, A.K. Gandhi, M.F. Waldman, C. Bjorklund, Y. Ning, D. Mendy, P. Schafer, A. Lopez-

Girona, S. Lentzsch, S.A. Schey, Y. Calle, R. Chelliah, R.Z. Orlowski, A. Madan, H. Avet-Loiseau, R. Chopra, Absence of mutations in cereblon (CRBN) and DNA damage-binding protein 1 (DDB1) genes and significance for IMiD therapy, Leukemia, 28 (2014) 1129-1131.
[8] G. Lu, R.E. Middleton, H. Sun, M. Naniong, C.J. Ott, C.S. Mitsiades, K.K. Wong, J.E. Bradner, W.G. Kaelin, Jr., The myeloma drug lenalidomide promotes the cereblon-dependent destruction of Ikaros proteins, Science, 343 (2014) 305-309.
[9] J. Kronke, N.D. Udeshi, A. Narla, P. Grauman, S.N. Hurst, M. McConkey, T. Svinkina, D. Heckl, E. Comer, X. Li, C. Ciarlo, E. Hartman, N. Munshi, M. Schenone, S.L. Schreiber, S.A. Carr, B.L. Ebert, Lenalidomide causes selective degradation of IKZF1 and IKZF3 in multiple myeloma cells, Science, 343 (2014) 301-305.
[10] M. Cavo, A third-generation IMiD for MM, Blood, 118 (2011) 2931-2932.
[11] R.J. Deshaies, Protein degradation: Prime time for PROTACs, Nat Chem Biol, 11 (2015) 634-635.
[12] A.R. Schneekloth, M. Pucheault, H.S. Tae, C.M. Crews, Targeted intracellular protein degradation induced by a small molecule: En route to chemical proteomics, Bioorg Med Chem Lett, 18 (2008) 5904-5908.
[13] S.W. Hicks, J.E. Galan, Hijacking the host ubiquitin pathway: structural strategies of bacterial E3 ubiquitin ligases, Curr Opin Microbiol, 13 (2010) 41-46.
[14] K. Cyrus, M. Wehenkel, E.Y. Choi, H. Swanson, K.B. Kim, Two-headed PROTAC: an effective new tool for targeted protein degradation, Chembiochem, 11 (2010) 1531-1534.
[15] M.S. Gadd, A. Testa, X. Lucas, K.H. Chan, W. Chen, D.J. Lamont, M. Zengerle, A. Ciulli, Structural basis of PROTAC cooperative recognition for selective protein degradation, Nat Chem Biol, 13 (2017) 514-521.
[16] K.M. Sakamoto, K.B. Kim, A. Kumagai, F. Mercurio, C.M. Crews, R.J. Deshaies, Protacs: chimeric molecules that target proteins to the Skp1-Cullin-F box complex for ubiquitination and degradation, Proc Natl Acad Sci U S A, 98 (2001) 8554-8559.
[17] C.M. Robb, J.I. Contreras, S. Kour, M.A. Taylor, M. Abid, Y.A. Sonawane, M. Zahid, D.J. Murry, A. Natarajan, S. Rana, Chemically induced degradation of CDK9 by a proteolysis targeting chimera (PROTAC), Chem Commun (Camb), 53 (2017) 7577-7580.
[18] A.C. Lai, M. Toure, D. Hellerschmied, J. Salami, S. Jaime-Figueroa, E. Ko, J. Hines, C.M. Crews, Modular PROTAC Design for the Degradation of Oncogenic BCR-ABL, Angew Chem Int Ed Engl, 55 (2016) 807-810.
[19] Y. Sun, X. Zhao, N. Ding, H. Gao, Y. Wu, Y. Yang, M. Zhao, J. Hwang, Y. Song, W. Liu, Y. Rao, PROTAC-induced BTK degradation as a novel therapy for mutated BTK C481S induced ibrutinib-resistant B-cell malignancies, Cell Res, 28 (2018) 779-781.
[20] M. Lu, T. Liu, Q. Jiao, J. Ji, M. Tao, Y. Liu, Q. You, Z. Jiang, Discovery of a Keap1-dependent peptide PROTAC to knockdown Tau by ubiquitination-proteasome degradation pathway, Eur J Med Chem, 146 (2018) 251-259.
[21] D.T. Saenz, W. Fiskus, Y. Qian, T. Manshouri, K. Rajapakshe, K. Raina, K.G. Coleman, A.P. Crew, A. Shen, C.P. Mill, B. Sun, P. Qiu, T.M. Kadia, N. Pemmaraju, C. DiNardo, M.S. Kim, A.J. Nowak, C. Coarfa, C.M. Crews, S. Verstovsek, K.N. Bhalla, Novel BET protein proteolysis-targeting chimera exerts superior lethal activity than bromodomain inhibitor (BETi) against post-myeloproliferative neoplasm secondary (s) AML cells, Leukemia, 31 (2017) 1951-1961.
[22] F. Jeanmougin, J.M. Wurtz, B. Le Douarin, P. Chambon, R. Losson, The bromodomain revisited, Trends Biochem Sci, 22 (1997) 151-153.
[23] L. Zeng, M.M. Zhou, Bromodomain: an acetyl-lysine binding domain, FEBS Lett, 513 (2002) 124-128.
[24] D. Houzelstein, S.L. Bullock, D.E. Lynch, E.F. Grigorieva, V.A. Wilson, R.S. Beddington, Growth and early postimplantation defects in mice deficient for the bromodomain-containing protein Brd4, Mol Cell Biol, 22 (2002) 3794-3802.
[25] U. Schaefer, Pharmacological inhibition of bromodomain-containing proteins in inflammation, Cold Spring Harb Perspect Biol, 6 (2014).
[26] A. Dey, F. Chitsaz, A. Abbasi, T. Misteli, K. Ozato, The double bromodomain protein Brd4 binds to acetylated chromatin during interphase and mitosis, Proc Natl Acad Sci U S A, 100 (2003) 8758-8763.
[27] D.S. Hewings, T.P. Rooney, L.E. Jennings, D.A. Hay, C.J. Schofield, P.E. Brennan, S. Knapp, S.J. Conway, Progress in the development and application of small molecule inhibitors of bromodomain-acetyl-lysine interactions, J Med Chem, 55 (2012) 9393-9413.
[28] A.C. Belkina, G.V. Denis, BET domain co-regulators in obesity, inflammation and cancer, Nat Rev Cancer, 12 (2012) 465-477.
[29] J. Lu, Y. Qian, M. Altieri, H. Dong, J. Wang, K. Raina, J. Hines, J.D. Winkler, A.P. Crew, K.

Coleman, C.M. Crews, Hijacking the E3 Ubiquitin Ligase Cereblon to Efficiently Target BRD4, Chem Biol, 22 (2015) 755-763.
[30] L. Bai, B. Zhou, C.Y. Yang, J. Ji, D. McEachern, S. Przybranowski, H. Jiang, J. Hu, F. Xu, Y. Zhao, L. Liu, E. Fernandez-Salas, J. Xu, Y. Dou, B. Wen, D. Sun, J. Meagher, J. Stuckey, D.F. Hayes, S. Li, M.J. Ellis, S. Wang, Targeted Degradation of BET Proteins in Triple-Negative Breast Cancer, Cancer Res, 77 (2017) 2476-2487.
[31] K. Raina, J. Lu, Y. Qian, M. Altieri, D. Gordon, A.M. Rossi, J. Wang, X. Chen, H. Dong, K. Siu, J.D. Winkler, A.P. Crew, C.M. Crews, K.G. Coleman, PROTAC-induced BET protein degradation as a therapy for castration-resistant prostate cancer, Proc Natl Acad Sci U S A, 113 (2016) 7124-7129.
[32] B. Zhou, J. Hu, F. Xu, Z. Chen, L. Bai, E. Fernandez-Salas, M. Lin, L. Liu, C.Y. Yang, Y. Zhao, D. McEachern, S. Przybranowski, B. Wen, D. Sun, S. Wang, Discovery of a Small-Molecule Degrader of Bromodomain and Extra-Terminal (BET) Proteins with Picomolar Cellular Potencies and Capable of Achieving Tumor Regression, J Med Chem, 61 (2018) 462-481.
[33] P. Ottis, C.M. Crews, Proteolysis-Targeting Chimeras: Induced Protein Degradation as a Therapeutic Strategy, ACS Chem Biol, 12 (2017) 892-898.
[34] P. Ottis, M. Toure, P.M. Cromm, E. Ko, J.L. Gustafson, C.M. Crews, Assessing Different E3 Ligases for Small Molecule Induced Protein Ubiquitination and Degradation, ACS Chem Biol, 12 (2017) 2570-2578.
[35] N. Mitsiades, C.S. Mitsiades, V. Poulaki, D. Chauhan, P.G. Richardson, T. Hideshima, N.C. Munshi, S.P. Treon, K.C. Anderson, Apoptotic signaling induced by immunomodulatory thalidomide analogs in human multiple myeloma cells: therapeutic implications, Blood, 99 (2002) 4525-4530.
[36] K.C. Carmony, K.B. Kim, PROTAC-induced proteolytic targeting, Methods Mol Biol, 832 (2012) 627-638.
[37] X. Zhou, L.X. Fan, D.J. Peters, M. Trudel, J.E. Bradner, X. Li, Therapeutic targeting of BET bromodomain protein, Brd4, delays cyst growth in ADPKD, Hum Mol Genet, 24 (2015) 3982-3993.
[38] M. Zengerle, K.H. Chan, A. Ciulli, Selective Small Molecule Induced Degradation of the BET Bromodomain Protein BRD4, ACS Chem Biol, 10 (2015) 1770-1777.
[39] C. Qin, Y. Hu, B. Zhou, E. Fernandez-Salas, C.Y. Yang, L. Liu, D. McEachern, S. Przybranowski, M. Wang, J. Stuckey, J. Meagher, L. Bai, Z. Chen, M. Lin, J. Yang, D.N. Ziazadeh, F. Xu, J. Hu, W. Xiang, L. Huang, S. Li, B. Wen, D. Sun, S. Wang, Discovery of QCA570 as an Exceptionally Potent and Efficacious Proteolysis Targeting Chimera (PROTAC) Degrader of the Bromodomain and Extra-Terminal (BET) Proteins Capable of Inducing Complete and Durable Tumor Regression, J Med Chem, 61 (2018) 6685-6704.
[40] D.P. Bondeson, B.E. Smith, G.M. Burslem, A.D. Buhimschi, J. Hines, S. Jaime-Figueroa, J. Wang, B.D. Hamman, A. Ishchenko, C.M. Crews, Lessons in PROTAC Design from Selective Degradation with a Promiscuous Warhead, Cell Chem Biol, 25 (2018) 78-87 e75.

Highlights

- We design and synthesize a novel IMiD analog TD-106
- TD-106 induces the degradation of IKZF1/3 and inhibits the proliferation of multiple myeloma cells *in vitro* as well as *in vivo*
- BET PROTAC with TD-106 efficiently induces the degradation of BET proteins, thereby inhibits cell proliferation.
- Collectively, TD-106 as a novel CRBN modulator can be used for targeted protein degradation.